ARTICLES
https://doi.org/10.1038/s41558-018-0088-y

nature climate change

Corrected: Author Correction

Under-estimated wave contribution to coastal sea-level rise

Angélique Melet[1*], Benoit Meyssignac[2], Rafael Almar[2] and Gonéri Le Cozannet[3]

Coastal communities are threatened by sea-level changes operating at various spatial scales; global to regional variations are associated with glacier and ice sheet loss and ocean thermal expansion, while smaller coastal-scale variations are also related to atmospheric surges, tides and waves. Here, using 23 years (1993–2015) of global coastal sea-level observations, we examine the contribution of these latter processes to long-term sea-level rise, which, to date, have been relatively less explored. It is found that wave contributions can strongly dampen or enhance the effects of thermal expansion and land ice loss on coastal water-level changes at interannual-to-multidecadal timescales. Along the US West Coast, for example, negative wave-induced trends dominate, leading to negative net water-level trends. Accurate estimates of past, present and future coastal sea-level rise therefore need to consider low-frequency contributions of wave set-up and swash.

Coastal zones and communities are expected to be increasingly threatened by sea-level changes acting at various timescales, ranging from episodic extreme events to interannual-to-centennial changes and rise linked to climate modes of variability and to climate change[1,2]. Related impacts include coastal erosion and shoreline retreat together with flooding of coastal areas, salt-water intrusion in the aquifers and surface water, and a potential decline of coastal wetlands such as mangroves and salt marshes[3,4]. The rise in coastal population, with half the world's population currently living within 60 km of the sea and three-quarters of all large cities located on the coast[5], is projected to increase in the future[6], thereby exposing an even larger part of the world's population to coastal hazards related to sea-level changes.

Changes in total water levels at the coast result from the superposition of global mean sea-level, regional sea-level and local sea-level changes (Fig. 1). Global mean sea-level variations are driven by ocean global warming and the transfer of water mass from the cryosphere and land to the ocean[7,8]. Departures from the global mean sea level are substantial at regional scales and essentially result from changes in ocean circulation and the associated ocean heat, salt and mass regional distribution[9,10]. Mass redistribution also leads to geoid changes that further impact regional sea-level variations[11]. Other processes make additional substantial contributions to total water-level changes in the coastal ocean: astronomical tides, atmospheric surges (here defined as changes due to surface atmospheric pressure and the displacement of surface waters by the wind, called wind set-up) and wave transformations in the surf zone (Fig. 1). The last includes wave set-up, which is the time-mean sea-level elevation onshore the wave breaking point due to wave energy dissipation, and swash, which corresponds to the vertical fluctuation of the water line above the still water level induced by individual waves. Wave set-up and swash induce different types of impact in particular during floods, through overtopping or overflowing. Overtopping occurs when individual waves pass over coastal defences or dunes because of swash. It results in a sporadic spillage of water on land. Overflowing happens when the mean water level is greater than the level of the land or defences, resulting in a continuous spillage of sea water on land. The expected impacts on the coast are considerably different in each case[12], with more rapid flooding induced by overflowing.

So far, most broad-scale studies of sea-level impacts have essentially focused on modelling tides and atmospheric surges and on the analysis of tide gauge extreme water levels[13,14]. Coastal processes, in particular waves, have been shown to be dominant contributors to extreme sea levels[15–18]. In contrast, few studies have analysed impacts of long-term (interannual and longer periods) sea-level changes on the coast, although at regional scales they have highlighted the importance of the wave contribution[19]. When performed at global scale, such long-term studies mostly overlook wave contributions[20]. However, there is increasing evidence for changes in wave regimes over the past decades related to changes in the surface winds in response to climate modes of variability[21,22]. Regional wave characteristics (height, direction and period) are also projected to change over large parts of the open ocean under future climate scenarios with increased greenhouse gas concentrations[23,24]. As wave set-up and swash depend on wave characteristics in the open ocean, they are also expected to change with climate modes of variability and under future climate scenarios. Sea-level changes induced by climate modes can be of the same order of magnitude for wave contributions and for thermal expansion and mass contributions. However, changes in waves in response to greenhouse gas emissions are expected to be more limited than changes due to the ocean thermal expansion and land ice mass loss as waves depend on atmospheric circulation by nature. The latter contributions will eventually dominate over the wave contribution in coastal total water levels, probably in the next decades to come. However, the time horizon at which this will happen is unknown.

In this study, we estimate at global scale the wave set-up and swash contributions to total water-level changes and rise at the coast at interannual-to-multidecadal timescales. Their contributions are compared with those of the other contributors to coastal total water-level change to determine where and at which timescales they are important contributors.

The scarcity of studies on interannual-to-multidecadal wave set-up and swash changes over the past decades is partly due to limitations of the observational system. Contemporary sea-level changes

[1]Mercator Ocean, Ramonville Saint Agne, France. [2]LEGOS, Université de Toulouse, CNES, CNRS, IRD, UPS, Toulouse, France. [3]BRGM / French Geological Survey, Orléans, France. *e-mail: amelet@mercator-ocean.fr

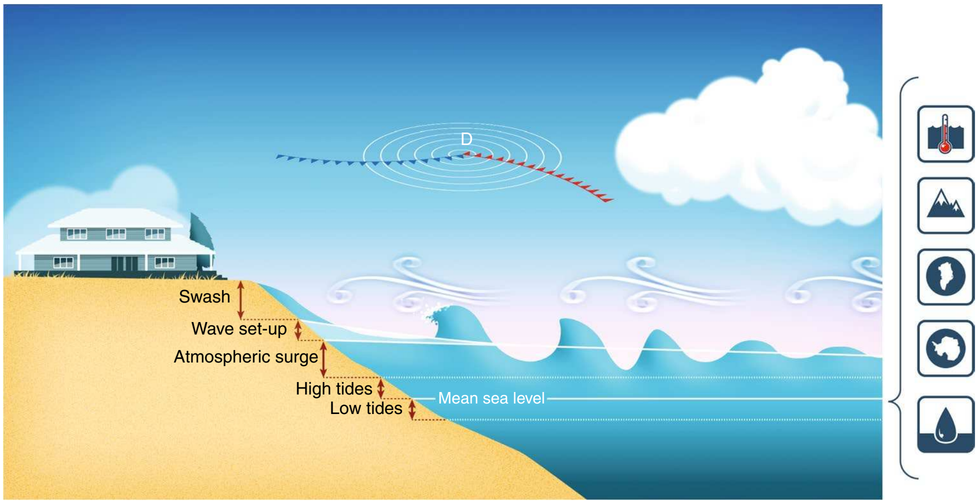

Fig. 1 | Schematic of processes contributing to total water-level changes at the coast. The mean sea level delivered in radar altimetry data includes contributions from ocean thermal expansion and ocean circulation, transfer of water from land to ocean due to mass loss from glaciers and from the Arctic and Antarctic ice sheets, as well as from land water storage changes (pictograms on the right, from top to bottom). Coastal processes including tides, atmospheric surges (due to atmospheric surface pressure effects and wind set-up) as well as wave set-up and swash also induce variations of total water level at the coast. D: depression.

have mainly been monitored through satellite radar altimetry and tide gauges. Satellite altimetry has provided measurements of sea-level changes since late 1992 and has given a clear and accurate picture of global and regional sea-level changes thereafter[25,26]. However, satellite long-term measurements of sea level are not reliable in the last 10–20 km off the coast[27,28]. Thus, they cannot observe the surf zone and capture nearshore wave set-up and swash. Tide gauges have provided records of coastal water-level changes for longer periods than altimetry (back to the eighteenth century at some sites of the Northern Hemisphere). Nevertheless, most of them are located in sheltered areas where the wave set-up signal is either dampened or negligible[29–32]. Direct observations of wave set-up and swash are usually performed through intensive in situ measurements covering periods of days to weeks.

Here, contributions to total (including the contribution from waves) water-level changes at the coast over 1993–2015 are estimated separately. The tidal contribution comes from a tidal model[33], and atmospheric surges are estimated from a barotropic ocean model[34] forced by atmospheric pressure and wind. Wind waves (short-period waves generated by the local winds) and swell waves (long-period waves remotely generated by the wind) set-up and swash are computed from a reanalysis[35] and parameterizations[36]. Global and regional sea-level changes induced by ocean thermal expansion and circulation, land ice mass loss and terrestrial water storage changes are estimated together from satellite radar altimetry data off the coasts. All these contributions to total water-level changes are estimated at 153 monitored coastal sites (Supplementary Fig. 1), which are approximately evenly distributed along the world's coastlines (except in polar regions) and for which tide gauges provide records spanning periods included in 1993–2015. Examples are given at two sites (Supplementary Fig. 1), in Supplementary Figs. 2 and 3. Individual contributions were summed to obtain the total water level at the coast, allowing us to assess the contribution of waves to total water-level rise and interannual-to-multidecadal changes at the coast.

Total water levels at the coast were compared with tide gauge data[37] (Supplementary Figs. 2–5). The comparison shows that, when excluding wave contributions, our estimates are highly correlated to tide gauge records (Supplementary Fig. 4). This indicates that processes other than waves are well captured in our estimates. When including wave contributions (which are only partly captured by tide gauge records, because they are located in sheltered areas), our estimates reproduce extreme events that are observed by tide gauges and other extreme events that are missed in the tide gauge records but that have been reported[30,32], giving confidence in the relevance of our estimated total water-level time series. At global scale, our estimated contributions show that the dominant contributors to sea-level extremes are waves and tides (Fig. 2 and Supplementary Information), confirming recent studies on the relative importance of contributors to water-level extremes[16,38].

Interannual-to-multidecadal changes

At interannual-to-multidecadal timescales (extracted through a low-pass filter with a cut-off frequency of 1.3 years; see Methods), regional wind and wave regimes change due to climate modes of variability[21]. These local and remote regional changes are conveyed to the coast through changes in wave height and period. Wave set-up and swash contributions to total water-level changes at the coast are shown in Fig. 3 together with the relative contributions of altimetry-derived sea level and atmospheric surges. Overall, the median contribution of waves to total water-level interannual-to-multidecadal variations across the 153 sites is as large as 58% (Supplementary Fig. 7) and is therefore also dominant at these timescales. This large contribution is distributed between swash and wave set-up (explaining, respectively, 38% and 20% of the variance). Globally, contributions from swells (36% of the variance) dominate those of wind waves (17%). The relative importance of wave contributions to low-frequency coastal total water-level changes is clearly regionally dependent. Wave contributions are more important at mid-to-high latitudes than in the tropics, except in the tropical Atlantic and central eastern tropical Pacific oceans (Fig. 3a). A stronger regional contribution from wind waves is noted in the Southern Ocean, central and western tropical Pacific and Caribbean islands (Fig. 3b) where winds are strong (westerlies in the Southern Ocean, trade winds in the tropics). By contrast, the contribution from swells is especially large at mid-latitudes along the western coasts of the Americas, Japan, the west and south coasts of Africa, the eastern tropical Indian Ocean. These regions correspond to coasts that are dominated by swell waves. Swells and wind waves tend to have more similar and dominant contributions to interannual-to-multidecadal total water-level changes in coastal sites under storm tracks, such as the northeastern Atlantic coasts.

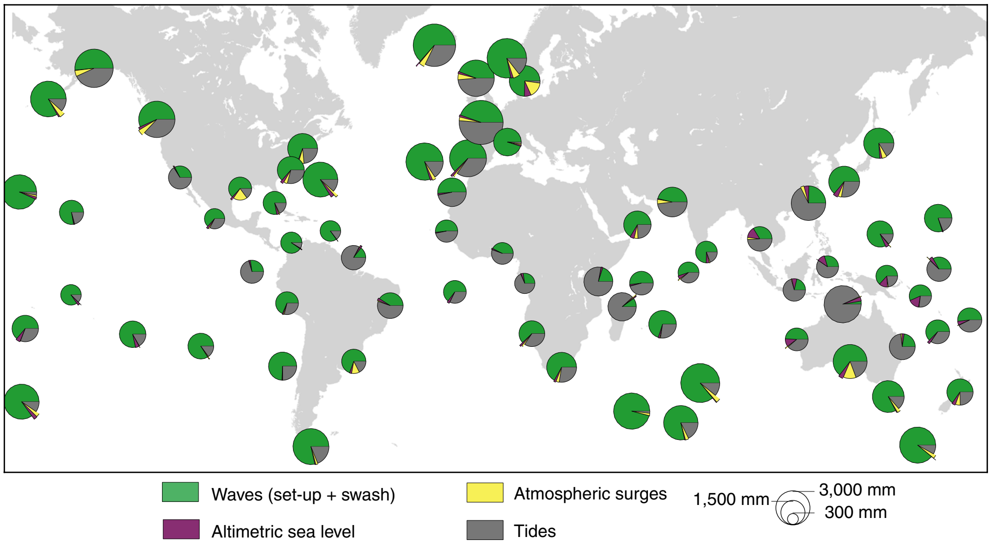

Fig. 2 | Contributions to extreme events. Pie charts of the relative contribution of waves (green), altimetry-derived sea level (violet), atmospheric surges (yellow) and tides (grey) to extreme total water levels. The size of the pie charts indicates the mean amplitude of extreme events. For clarity, results are shown for a subset of 72 sites. Results for the 153 sites are shown in Supplementary Fig. 6.

In the Indo-Pacific tropics, the global and regional sea-level variations measured by altimetry are the main contributors to interannual-to-multidecadal total water-level variations at the coast (Fig. 3a). The very large contribution of the altimetric sea level in these regions is mostly related to the strong regional sea-level signature of climate modes such as the El Niño / Southern Oscillation (ENSO), the Pacific Decadal Oscillation (PDO) and the Indian Ocean Dipole on the thermal expansion of the ocean[39]. The signal then propagates along the surrounding coasts through Kelvin waves (see the coasts of Western Australia, Sumatra and California). In the tropical Atlantic, dominant climate modes such as the Atlantic meridional mode induce weaker sea-level variations than the ENSO or PDO in the tropical Indo-Pacific ocean[40,41]. Together with energetic swells originating from the Southern Ocean and impinging on the coasts of the eastern tropical Atlantic[42], these explain the dominance of waves on total water-level changes at interannual-to-multidecadal timescales in this region's coastline.

Tides do not substantially contribute to interannual-to-multidecadal total water-level changes (Fig. 3a), as the modulation of tides is small at these frequencies[43]. The contribution of atmospheric surge to interannual-to-multidecadal total water-level changes at the coast is sizeable compared with the altimetric sea-level contribution at high latitudes and in the northeastern Atlantic (Fig. 3a), expressing at the coast the low modulation of storminess, sea-level pressure and surface wind patterns.

The contribution of wave set-up to interannual-to-multidecadal water-level changes at the coast is further directly compared with the contributions of processes influencing the time-mean water level in the coastal zone: altimetric sea level and atmospheric surges (Fig. 3 and Supplementary Fig. 7). The time variability of the wave set-up makes a sizeable contribution to interannual-to-multidecadal mean water-level changes at the coast. Indeed, changes in the wave set-up amplitude reach the same order of magnitude or even exceed the contribution due to the variability of ocean thermal expansion, land ice loss and ocean circulation in large parts of the global ocean. In the Southern Ocean and western tropical Atlantic, wind-wave-induced set-up is larger than the contribution from altimetric sea level. This large contribution is related to interannual-to-multidecadal modulations of strong local winds at regional scales (westerlies in the Southern Ocean and trade winds in the tropical Atlantic) in response to climate modes such as the Southern Annular Mode, ENSO and PDO[22,44]. Wind-wave-induced set-up also largely contributes to water-level variations at the coast at these timescales in the tropical Pacific due to the modulation of trade winds[45]. Changes in waves generated in the Southern Ocean affect wave characteristics and induced set-up over large parts of the global ocean through the northward propagation of swells in the other ocean basins[21,23]. Swell-induced set-up indeed shows an important contribution to interannual-to-multidecadal total water-level changes at the coast in the South Atlantic and eastern Pacific, particularly along thewestern coasts of the United States and Chile. In the northeastern Atlantic, wave set-up largely exceeds the contribution from thermal expansion, ocean circulation and ocean mass changes captured by altimetry, with a contribution from both wind waves and swells (Fig. 3b). Interannual-to-multidecadal changes in wave characteristics in this region are notably related to the North Atlantic Oscillation.

Wave contributions are therefore found to be dominant contributors to interannual-to-multidecadal total water-level changes over large parts of the world's coastlines.

Trends

We now investigate whether waves also substantially contribute to lower frequencies, by assessing their relative contribution to total water-level rise at the coast over 1993–2015. Large spatial variability of total water-level rise at the coast and of its contributors is found (Fig. 4). Ocean thermal expansion and the transfer of water from land to ocean (altimetry-derived sea level) generally dominate coastal water-level rise over 1993–2015. However, waves make substantial contributions to coastal total water-level rise, resulting in a substantial increase (for example, the western tropical Pacific and tropical South Atlantic) or in several places dampening or reversal of the trends due to ocean thermal expansion, ocean circulations and transfer of liquid/solid water from land to ocean (for example, Japan, the North Sea and the northeastern Pacific). Trends in swell wave contributions even largely dominate the coastal total water-level trends along the western coast of the United States, leading to negative net trends.

Around Japan and Europe as well as in the western tropical Pacific and tropical Atlantic, the trend in wave contributions

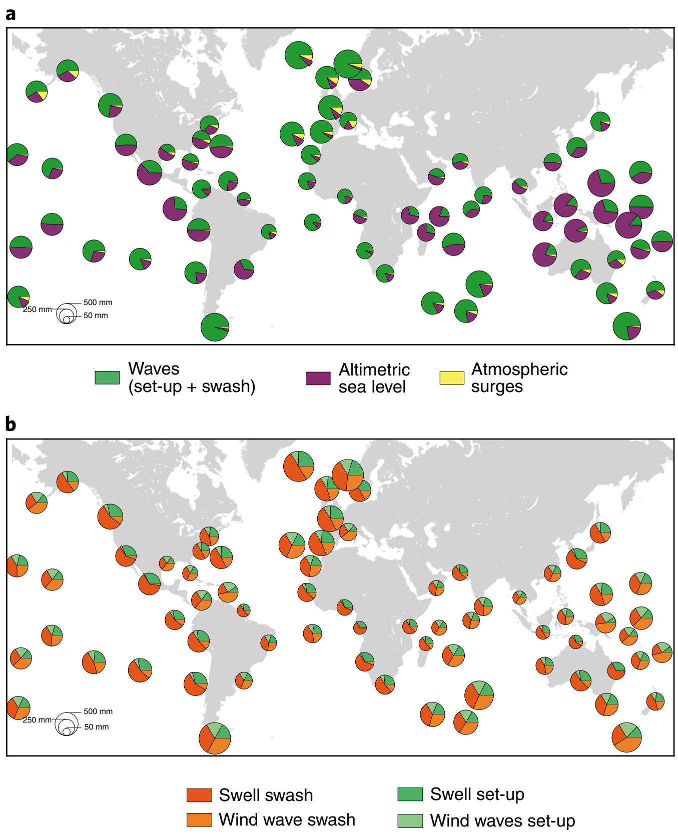

Fig. 3 | Contribution to interannual-to-multidecadal total water-level variations. a, Pie charts of the relative contribution of waves (sum of swell and wind wave swash and set-up) (green), altimetry-derived sea level (violet) and atmospheric surges (yellow) to total water-level detrended interannual-to-multidecadal variations. **b**, Pie charts of the relative contribution of swell set-up (dark green), wind wave set-up (light green), swell swash (dark orange) and wind wave swash (light orange) to the wave-induced detrended interannual-to-multidecadal water-level variations. The size of the pie charts indicates the standard deviation of detrended interannual-to-multidecadal sea-level variations. Scalings are indicated on the lower left corner of the panels. For clarity, results are shown for a subset of 72 sites. Results for the 153 sites are shown in Supplementary Fig. 7.

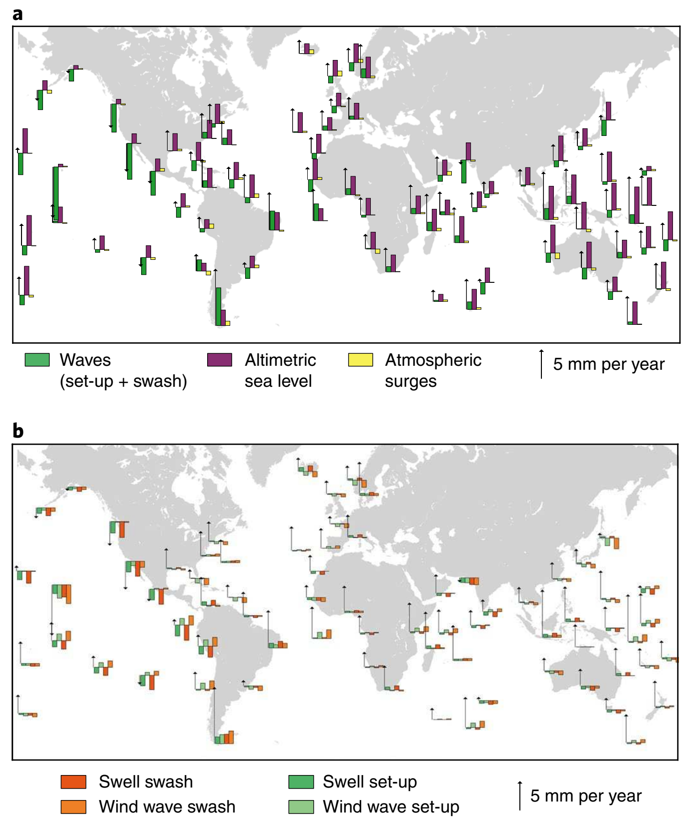

Fig. 4 | Contribution to total water-level trends. a, Coastal total water-level trends due to waves (green), altimetry-derived sea level (violet) and atmospheric surges (yellow) over 1993–2015. **b**, Decomposition of the wave-induced total water-level trends into swell set-up (dark green), wind wave set-up (light green), swell swash (dark orange) and wind wave swash (light orange) trends. The total trend at each site (sum of the trends of all contributors) is indicated as a black arrow. For clarity, results are shown for a subset of 72 sites. Results for the 153 sites are shown in Supplementary Fig. 8.

is induced by trends in local winds: the mid-latitudes westerlies and the trade winds[46]. Winds over the Southern Ocean have strengthened since 1993, consistent with the increasing trend in the Southern Annular Mode[22]. Pacific trade winds also accelerated over the past two decades[47]. Such trends could be long-term trends as climate models project a probable poleward shift of the storm tracks and an increase in trade winds[23,24]. This indicates that some regions could be more exposed (and others less exposed) to sea-level rise in response to climate change than expected, as wave contributions are not yet taken into account in climate projections of coastal water-level changes over the next century.

Discussion

A first-order estimate of the importance of waves in total water-level changes and rise at the coast at interannual-to-multidecadal timescales is provided at global scale. Although large uncertainties exist regarding wave contribution to total water level at the coast (Supplementary Figs. 6–8), estimates of the contributions to total water-level changes along open coasts robustly indicate that waves are important not only in explaining water-level extremes. Despite waves being transient by nature, they are also major contributors to interannual-to-multidecadal total water-level changes at the coast due to the low-frequency modulation of their characteristics related to wind changes. This result is regionally dependent, but for some regions, the wave contribution can mask or enhance the effect of thermal expansion and ice mass transfer from land over unexpectedly long periods of several decades.

This main result has far-reaching implications: it advocates for an inclusion of the wave contributions in past, contemporary and future low-frequency sea-level changes at the coast. Indeed, waves will very probably contribute to future multidecadal water-level rise (for example, horizons of 2030, 2050 and longer) due to interannual-to-multidecadal changes in wind patterns induced by both climate modes of variability and climate change. Wave-driven contributions to coastal total water-level changes have been mostly related to climate modes of variability over the past two decades (Supplementary Fig. 9), reaching amplitudes comparable to thermal expansion and mass contributions. Regarding trends, wave-driven water-level rise along open coasts over the past two decades evidenced here modulates or even dominates the contributions of processes currently taken into account in decadal predictions and future long-term changes in sea level (including ocean thermal expansion, heat, salt and mass redistributions by ocean circulations, and transfer of water from land to ocean[7,48]). In addition, some robust patterns of longer-term wave-regime changes emerge in climate change projections[23]. In particular, a strengthening of the westerlies in the Southern Ocean and of the trade winds in the tropical oceans is projected in response to climate change. As changes in local wave regimes could also impact remote regions via swell propagation, trends in wave-driven contributions to total water level at the coast could persist over parts of the global ocean in response to climate change. Since wave-induced water-level rise in response to greenhouse gases is related to changes in atmospheric circulation, it will be more limited than sea-level rise due to combined thermal expansion and land ice mass transfer to the ocean. The latter is indeed expected to continue for centuries as it is limited only by the amount of heat excess in the climate system that can be stored in the ocean, and by the amount of land water that can potentially be transferred to the ocean from glaciers and ice sheets. However, wave contributions could be sizeable for long-term coastal total water-level changes as long as sea-level rise remains limited to a few millimetres per year. Given the uncertainties in current sea-level projections, this could cover time periods ranging from multi-decadal (2030–2050) to centennial (2100) timescales that are more relevant for sea-level projections and associated decision making. As the frequency of marine flooding events is expected to grow drastically over the coming decades due to a committed sea-level rise of a few tens of centimetres, our results indicate that accounting for wave contributions to long-term coastal total water-level changes can lead to more accurate decadal predictions and longer-term projections of total water level at the coast.

As for global-scale projections of future extreme water levels, the traditional approach used to date consists of observing or modelling past extreme water levels, mostly through extreme value analysis methods. The contemporary return levels are then quantified and used to estimate future changes in exceedance probabilities by vertically shifting the return levels by the projected sea-level change (which only includes changes in the steric, dynamical and mass sea-level contributions[7]). These approaches assume that wave climate is stationary while climate is changing[16]. Studies accounting for the evolution of wave conditions under climate change and for their interactions with sea-level rise are emerging only at regional scales[49,50]. Our results further advocate for the inclusion of non-stationary wave conditions in future global studies.

Methods

Methods, including statements of data availability and any associated accession codes and references, are available at https://doi.org/10.1038/s41558-018-0088-y.

Received: 18 September 2017; Accepted: 24 January 2018;
Published online: 26 February 2018

References

1. Wong, P. P. et al. In *Climate Change 2014: Impacts, Adaptation, and Vulnerability* (eds Field, C. B. et al.) 361–409 (IPCC, Cambridge Univ. Press, 2014).
2. Hallegatte, S., Green, C., Nicholls, R. J. & Corfee-Morlot, J. Future flood losses in major coastal cities. *Nat. Clim. Change* **3**, 802–806 (2013).
3. Nicholls, R. J. & Cazenave, A. Sea-level rise and its impact on coastal zones. *Science* **328**, 1517–1520 (2010).
4. Brown, S. et al. In *Coastal Hazards* 117–149 (Springer, Dordrecht, 2013).
5. McGranahan, G., Balk, D. & Anderson, B. The rising tide: assessing the risks of climate change and human settlements in low elevation coastal zones. *Environ. Urban.* **19**, 17–37 (2007).
6. Hugo, G. Future demographic change and its interactions with migration and climate change. *Glob. Environ. Change* **21**, S21–S33 (2011).
7. IPCC *Climate Change 2013: The Physical Science Basis* (eds Stocker, T. F. et al.) Ch. 13 (Cambridge Univ. Press, 2013).
8. Slangen, A. B. et al. Evaluating model simulations of twentieth-century sea level rise. Part I: Global mean sea level change. *J. Clim.* **30**, 8539–8563 (2017).
9. Forget, G. & Ponte, R. M. The partition of regional sea level variability. *Progress. Oceanogr.* **137**, 173–195 (2015).
10. Meyssignac, B. et al. Evaluating model simulations of twentieth-century sea-level rise. Part II: Regional sea-level changes. *J. Clim.* **30**, 8565–8593 (2017).
11. Tamisiea, M. E. Ongoing glacial isostatic contributions to observations of sea level change. *Geophys. J. Int.* **186**, 1036–1044 (2011).
12. Sallenger, A. H. Storm impact scale for barrier islands. *J. Coast. Res.* **16**, 890–895 (2000).
13. Muis, S., Verlaan, M., Winsemius, H. C., Aerts, J. C. & Ward, P. J. A global reanalysis of storm surges and extreme sea levels. *Nat. Commun.* **7**, 11969 (2016).
14. Woodworth, P. L. et al. Towards a global higher-frequency sea level dataset. *Geosci. Data J.* **3**, 50–59 (2016).
15. Woodworth, P., Gregory, J. & Nicholls, R. in *The Sea* (eds Robinson, A. R. & Brink, K.) Vol. 13 (Harvard Univ. Press: Harvard, 2004).
16. Vitousek, S. et al. Doubling of coastal flooding frequency within decades due to sea-level rise. *Sci. Rep.* **7**, 1399 (2017).
17. Serafin, K. A., Ruggiero, P. & Stockdon, H. F. The relative contribution of waves, tides, and non-tidal residuals to extreme total water levels on US West Coast sandy beaches. *Geophys. Res. Lett.* **44**, 1839–1847 (2017).
18. Rueda, A. et al. Global classification of coastal flooding climates. *Sci. Rep.* **7**, 5038 (2017).
19. Ruggiero, P. Is the intensifying wave climate of the US Pacific Northwest increasing flooding and erosion risk faster than sea level rise? *J. Waterw. Port. Coast. Ocean Eng.* **139**, 88–97 (2013).
20. Nicholls, R. J. et al. Sea-level scenarios for evaluating coastal impacts. *WIREs Clim. Change* **5**, 129–150 (2014).
21. Semedo, A., Suselj, K., Rutgersson, A. & Sterl, A. A global view on the wind sea and swell climate and variability from ERA-40. *J. Clim.* **24**, 1461–1479 (2011).
22. Young, I. R., Zieger, S. & Babanin, A. V. Global trends in wind speed and wave height. *Science* **332**, 451–455 (2011).
23. Hemer, M. A., Fan, Y., Mori, N., Semedo, A. & Wang, X. L. Projected future changes in wind-wave climate in a multi-model ensemble. *Nat. Clim. Change* **3**, 471–476 (2013).
24. Wang, X. L., Feng, Y. & Swail, V. R. Changes in global ocean wave heights as projected using multimodel CMIP5 simulations. *Geophys. Res. Lett.* **41**, 1026–1034 (2014).
25. Cazenave, A. et al. The rate of sea-level rise. *Nat. Clim. Change* **4**, 358–361 (2014).
26. Ablain, M. et al. Improved sea level record over the satellite altimetry era (1993–2010) from the Climate Change Initiative project. *Ocean Sci.* **11**, 67–82 (2015).
27. Cipollini, P., Calafat, F. M., Jevrejeva, S., Melet, A. & Prandi, P. Monitoring sea level in the coastal zone with satellite altimetry and tide gauges. *Surv. Geophys.* **38**, 33–57 (2017).
28. Birol, F. et al. Coastal applications from nadir altimetry: example of the X-TRACK regional products. *Adv. Space Res.* **59**, 936–953 (2017).
29. Thompson, R. O. & Hamon, B. V. Wave setup of harbor water levels. *J. Geophys. Res.* **85**, 1151–1152 (1980).
30. Hoeke, R. K. et al. Widespread inundation of Pacific islands triggered by distant-source wind-waves. *Glob. Planet. Change* **108**, 128–138 (2013).
31. Hoeke, R. K., McInnes, K. L. & O'Grady, J. G. Wind and wave setup contributions to extreme sea levels at a tropical high island: a stochastic cyclone simulation study for Apia, Samoa. *J. Mar. Sci. Eng.* **3**, 1117–1135 (2015).
32. Melet, A., Almar, R. & Meyssignac, B. What dominates sea level at the coast: a case study for the Gulf of Guinea. *Ocean Dyn.* **66**, 623–636 (2016).
33. Carrère, L., Lyard, F., Cancet, M., Guillot, A. & Roblou, L. FES2012: a new global tidal model taking advantage of nearly 20 years of altimetry. In *Proc. 20 Years Prog. Radar Altimetry Symp.* (ed. Ouwehand, L.) 710–781 (European Space Agency, Noordwijk, 2013).
34. Carrère, L. & Lyard, F. Modeling the barotropic response of the global ocean to atmospheric wind and pressure forcing-comparisons with observations. *Geophys. Res. Lett.* **30**, 1275 (2003).
35. Dee, D. P. et al. The ERA-Interim reanalysis: configuration and performance of the data assimilation system. *Q. J. R. Meteorol. Soc.* **137**, 553–597 (2011).
36. Stockdon, H. F., Holman, R. A., Howd, P. A. & Sallenger, A. H. Empirical parameterization of setup, swash, and runup. *Coast. Eng.* **53**, 573–588 (2006).
37. Caldwell, P. C., Merrifield, M. A. & Thompson, P. R. *Sea Level Measured by Tide Gauges from Global Oceans—the Joint Archive for Sea Level Holdings (NCEI Accession 0019568)* Version 5.5 (NOAA National Centers for Environmental Information, 2015).
38. Merrifield, M. A., Genz, A. S., Kontoes, C. P. & Marra, J. J. Annual maximum water levels from tide gauges: contributing factors and geographic patterns. *J. Geophys. Res.* **118**, 2535–2546 (2013).
39. Roberts, C. et al. On the drivers and predictability of seasonal-to-interannual variations in regional sea level. *J. Clim.* **29**, 7565–7585 (2016).
40. Bilbao, R. A. F., Gregory, J. M. & Bouttes, N. Analysis of the regional pattern of sea level change due to ocean dynamics and density change for 1993–2099 in observations and CMIP5 AOGCMs. *Clim. Dyn.* **45**, 2647–2666 (2015).
41. Piecuch, C. G. & Ponte, R. M. Buoyancy-driven interannual sea level changes in the tropical South Atlantic. *J. Phys. Oceanogr.* **43**, 533–547 (2013).

42. Almar, R. et al. Response of the Bight of Benin (Gulf of Guinea, West Africa) coastline to anthropogenic and natural forcing, part 1: wave climate variability and impacts on the longshore sediment transport. *Cont. Shelf Res.* **110**, 48–59 (2015).
43. Woodworth, P. L. A note on the nodal tide in sea level records. *J. Coast. Res.* **28**, 316–323 (2012).
44. Swart, N. C. & Fyfe, J. C. Observed and simulated changes in the Southern Hemisphere surface westerly wind-stress. *Geophys. Res. Lett.* **39**, L16711 (2012).
45. Merrifield, M. A., Thompson, P. R. & Lander, M. Multidecadal sea level anomalies and trends in the western tropical Pacific. *Geophys. Res. Lett.* **39**, L13602 (2012).
46. Bengtsson, L., Hodges, K. & Keenlyside, N. Will extratropical storms intensify in a warmer climate? *J. Clim.* **22**, 2276–2301 (2009).
47. Takahashi, C. & Watanabe, M. Pacific trade winds accelerated by aerosol forcing over the past two decades. *Nat. Clim. Change* **6**, 768–772 (2016).
48. Slangen, A. B. A. et al. Projecting twenty-first century regional sea-level changes. *Clim. Change* **124**, 317–332 (2014).
49. Vousdoukas, M. I., Mentaschi, L., Voukouvalas, E., Verlaan, M. & Feyen, L. Extreme sea levels on the rise along Europe's coasts. *Earth's Future* **5**, 304–323 (2017).
50. Arns, A. et al. Sea-level rise induced amplification of coastal protection design heights. *Sci. Rep.* **7**, 40171 (2017).

Acknowledgements
The authors are grateful to all people and institutions who provided data used in this study, including F. Lyard for providing FES2014 tidal data. R.A. received support from French grants through ANR (COASTVAR ANR-14-ASTR-0019). B.M. and G.L.C. received funding from the ECLISEA (European advances on CLImate services for coasts and SEAs) project, funded through the ERA4CS (European Research Area for Climate Services) framework. This work was supported by the CNES (Centre National d'Etudes Spatiales). It is based on observations from the Topex/Poseidon and Jason 1/2 missions. This work is a contribution to the LEFE/IMPHALA project.

Author contributions
A.M. performed the analysis, created all figures and wrote the early drafts and final version of the manuscript. A.M., B.M. and R.A. participated in the elaboration of the study and early drafts. R.A. computed the contributions from waves. All authors participated in the interpretation of the results, in text revisions and in the final versions of the manuscript.

Competing interests
The authors declare no competing interests.

Additional information
Supplementary information is available for this paper at https://doi.org/10.1038/s41558-018-0088-y.

Reprints and permissions information is available at www.nature.com/reprints.

Correspondence and requests for materials should be addressed to A.M.

Publisher's note: Springer Nature remains neutral with regard to jurisdictional claims in published maps and institutional affiliations.

Methods

Coastal sites. We selected 153 coastal sites (Supplementary Fig. 1). The selection was based on the availability of Global Sea Level Observing System tide gauge records (which provide an approximately evenly distributed sampling of coastal sea-level variations). From the Global Sea Level Observing System dataset, a subset of tide gauges was selected to remove tide gauges in highly sampled regions where results were consistent with neighbouring tide gauges. Tide gauge data were downloaded from the University of Hawaii Sea Level Center (https://uhslc.soest.hawaii.edu/data).

Time series of contributors to sea level at the coast. Each contribution to total water-level changes at the coast was evaluated separately over the period 1993–2015, following the methodology developed at a pilot site[32] (Cotonou, Republic of Benin), which combines state-of-the-art models and datasets that have been validated in previous studies.

Altimetric sea-level time series were extracted from the gridded daily altimetric sea-level maps produced by the SSALTO/DUACS (*Segment Sol multi-missions d'ALTimetrie, d'Orbitographie et de localisation précise* / Data Unification and Altimeter Combination System)[51] and distributed by the Copernicus Marine Environment Monitoring Service using the closest points to the coastal sites. The uncertainty in local altimetric measures at 1 Hz is of the order of 1–2 cm, and the regional sea-level trend uncertainty is of the order of 2–3 mm per year (ref. [26]). Atmospheric surges were extracted from the dynamical atmospheric correction applied to altimetric data, provided by the MOG2D-G (Modèle aux Ondes de Gravité 2-Dimensions Global; 2D Gravity Wave Model) barotropic model[34] forced by the ERA-Interim (European Centre for Medium-Range Weather Forecasts Reanalysis Interim) winds and the inverted barometer effect with data outputs at a six-hourly frequency. Due to the low resolution of the barotropic model, atmospheric surges induced by small-scale hurricanes are not accounted for in our estimates of extreme events. In addition, extreme wind events are poorly captured by the atmospheric reanalysis[35].

No additional coastal wind set-up was applied, as this effect is small for sites facing narrow continental shelves, and is considered resolved in the MOG2D-G model over large continental shelves. Tides at the coastal sites are provided hourly by the FES2014 (Finite Element Solution 2014) tidal model[33].

Wind wave and swell wave set-up and swash are estimated separately six-hourly from state-of-the-art formulations[36]:

$$\text{swash} = \frac{1.1}{2}\left(L_0 H_0 \left(0.5625\beta^2 + 0.004\right)\right)^{1/2} \tag{1}$$

$$\text{set-up} = 0.385\beta\sqrt{L_0 H_0} \tag{2}$$

where H_0 and L_0 are the deep-water wave height and wavelength, respectively, extracted from the ERA-Interim[35], and β is a slope parameter. These formulations have been developed for use on natural beaches over a wide range of conditions. They have been calibrated using shoreline water-level time series collected during ten dynamically diverse field experiments and have been evaluated[36]. It should, however, be noted that the set-up and swash formulations remain largely untested and unvalidated for many of the types of locations to which the formula is being applied here (for example, semi-enclosed bays prone to an environmental wave set-up, and steep-shelfed small islands with fringing reefs[52]). The foreshore bathymetry slope parameter β was set to 0.1 globally, which is a reasonable estimate, although it may vary substantially in space and time[53]. Sensitivity tests to this value are provided below and in Supplementary Figs. 6b, 7b and 8b. Sensitivity tests to the formulations of wave set-up and swash are provided below and in Supplementary Figs. 6c, 7c and 8c.

Interactions between the different contributors to sea-level changes are disregarded, but are expected to be more important for extreme events than for interannual-to-multidecadal sea-level rise. Accounting for these interactions should not qualitatively change the main results of this study. Interactions between tides and sea level, for instance, are not thought to exceed 15% of the total water level along western European coasts, which are among the most exposed to those processes[54]. However, nonlinear interactions between waves and the underlying water depth might affect total water-level variations at the coast, including at interannual-to-multidecadal timescales, and total water-level trends[50].

Vertical land motions such as these induced by glacial isostatic adjustment, which can be important for some coastal sites (for example, northeastern coast of the United States, and Scandinavian sites), are disregarded here.

Interannual-to-multidecadal variations are isolated from the detrended and deseasonalized time series by using a Hamming low-pass filter with a cut off of 1.3 years. Trends are extracted through a linear regression of the time series. Daily estimates are used for diagnostics on the contributions to interannual-to-multidecadal variability and trends. Extreme events are defined as the highest 2% of the total sea-level time series (using the 98th percentile of the sea-level distribution), with extreme events being separated by at least three days to ensure one specific event is selected only once. Results are not sensitive to the use of a declustering period of seven days instead of three days (not shown).

To study extreme events, hourly estimates are used (using linear interpolation for contributors that are provided at lower frequencies).

To show that our approach, using a combination of observations and models, can explain the local tide gauge records (when waves are removed), figures of the sea-level change contributors time series together with tide gauge records are presented at two contrasted sites (Supplementary Fig. 1), in Supplementary Figs. 2 and 3. Another example can be found for Cotonou, Republic of Benin[32]. These figures show a good agreement between the tide gauge records and our water-level time series (when waves are removed, Supplementary Figs. 2j and 3j), which validates the sum of all contributions to sea level at the coast except waves. A systematic quantitative validation of wave contributions is currently not possible as the scientific community is lacking long enough time series of wave set-up and swash. Indeed, no observing system currently provides continuous observations from the coast to the open ocean. New observational systems are being implemented, such as video monitoring, but over only a few sites worldwide. Moreover, this recent monitoring does not yet allow analysis of interannual to long-term changes. However, the results presented here are regionally consistent with the spatial patterns of wave energy and altimetric sea-level variability, trends and extremes.

Comparisons with tide gauge records. Our estimated time series of water level at the coast were compared with tide gauge records. Correlations between our estimates of water level at the coast and tide gauge data confirm that wave-induced components are not entirely captured by the tide gauges (Supplementary Fig. 4). Indeed, wave-induced components are maximum at open wave-exposed coasts. Depending on their position relative to the surf zone and whether they are located in sheltered environments such as harbours, tide gauges only partially capture wave set-up. In addition, tide gauges are not designed to capture the swash. When wave contributions are accounted for in our estimates of total water level at the coast, correlations with tide gauge records are spatially heterogeneous and reach only 0.63 ± 0.21 (Supplementary Fig. 4a). However, when wave contributions are discarded from our estimates, correlations are more spatially uniform and largely increase, to 0.96 ± 0.05 (Supplementary Fig. 4b). This indicates that tide gauge records are more representative of processes other than wave set-up and swash, and that the water-level signature of processes captured by tide gauges is well reproduced in our estimates (as further shown in Supplementary Figs. 2 and 3).

However, comparisons of the time series confirm that tide gauge records partly missed extreme events that are captured by our estimates and that have been reported[30,32]. This indicates that our estimates of total water level at the coast are more relevant to studying sea-level impacts than tide gauge records.

Correlations between our estimates of water level at the coast (excluding wave contributions) and tide gauge data at interannual-to-multidecadal timescales were performed for tide gauges with records longer than seven years and reach 0.79 ± 0.26 (Supplementary Fig. 4c). This confirms that our estimates capture the interannual-to-multidecadal variability observed in tide gauge records, which is dominated by the interannual-to-multidecadal variability observed in altimetry-derived sea level.

Root mean squared deviations (r.m.s.d.) between our estimates of water level at the coast and tide gauge data have a mean and standard deviation of 84 mm ± 31 mm across the 153 coastal sites. They range from 31 mm to 176 mm (Supplementary Fig. 5a). The r.m.s.d. represent 24 ± 18% of the r.m.s. of the water-level estimates over the tide gauge record periods across the 153 coastal sites (Supplementary Fig. 5b). The r.m.s.d. were also computed for the percentile intervals 0–2, 2–10, 10–90, 90–98 and 98–100 and found to be of similar amplitude (with means ranging from 79 mm to 84 mm, and a standard deviation of 31 mm across the 153 coastal sites).

Uncertainties in wave contributions. Although our results are subject to different sources of uncertainties (interactions between the different contributors are disregarded, the nearshore bathymetry is uncertain, and uncertainties exist in the datasets and parameterizations used), the sensitivity tests that we performed (Supplementary Figs. 6–8) indicate that our results are qualitatively robust. Therefore, our methodology is well suited for studying the total water level at the coast on short to long timescales over the world's coastlines, awaiting for global-ocean–wave–atmosphere–tide coupled reanalyses and more accurate coastal remote sensing.

Uncertainties related to the wave reanalysis. Deep-water wave height and wavelength are extracted from the ERA-Interim reanalysis. ERA-interim is consistent through time and is suitable for multi-year analysis[55]. However, ERA-Interim tends to under-estimate significant wave height, especially when due to tropical cyclones[55]. Thus, our estimates probably under-estimate the full range of wave excursions. Moreover, several studies have noted the uncertainties arising from trends in reanalysis products that are not replicated in in situ measurements or satellite-derived trends[56,57].

Sensitivity to the wave set-up and swash formulation. Uncertainties related to the wave set-up and swash parameterizations are estimated by using two other available formulations ((ii) and (iii) below) in addition to the reference formulations (i) used in this study:

(i) Up-to-date and reference formulation[17,36] relevant for a wide range of conditions:

$$\text{swash} = \frac{1.1}{2}\left(L_0 H_0 \left(0.5625\beta^2 + 0.004\right)\right)^{1/2} \tag{3}$$

$$\text{set-up} = 0.385\beta\sqrt{L_0 H_0} \tag{4}$$

(ii) Formulation based on previous estimates for wave set-up[58] and swash[59,60] and used for the development of the methodology at a pilot site[32]:

$$\text{swash} = \frac{1.37}{2}\left(0.757\beta^2 L_0 H_0 - 0.167\beta H_0\sqrt{L_0 H_0} + 0.044 H_0^2\right)^{1/2} \tag{5}$$

$$\text{set-up} = 0.45\beta\sqrt{L_0 H_0} \tag{6}$$

(iii) Simplified formulation relevant only for dissipative beaches[16,36]:

$$\text{swash} = 0.027\sqrt{L_0 H_0} \tag{7}$$

$$\text{set-up} = 0.016\sqrt{L_0 H_0} \tag{8}$$

Supplementary Figs. 6c, 7c and 8c show that waves are dominant contributors to total water-level extremes and to interannual-to-multidecadal total water-level changes at the coast, and make substantial contributions to coastal water-level rise regardless of the formulations used to estimate wave set-up and swash. Wave contribution to interannual-to-multidecadal water-level changes ranges between 28% and 58% on average over the 153 coastal sites. On average, swell contribution to the total wave contribution are of 64% for all three formulations. The contribution from swell and wind wave set-up is more similar to the contribution from swell and wind wave swash for formulation (ii) (41% and 59% of the total wave contribution, respectively) than for both formulation (i) (34% and 66% of the total wave contribution, respectively) and formulation (iii) (25% and 75% of the total wave contribution, respectively).

Sensitivity to the beach slope. To evaluate wave set-up and swash, a constant uniform value of 0.10 for the beach slope parameter β was used (formulation (i)). Although this is a realistic mean value for the world's coastlines[53], beach slopes evolve both spatially and temporally[61]. To test the sensitivity of the contribution of waves to total water-level changes at the coast to the beach slope parameter, we estimated the relative contributions of drivers of water-level changes when the beach slope parameter was increased or decreased by 20% (leading to slopes of 0.12 and 0.08, respectively) and by 50% (leading to slopes of 0.15 and 0.05, respectively; note that a slope of 0.15 is not unrealistic, but lies beyond the applicability range of formulation (i) used in this study). The relative contributions of waves to the total water level at the coast estimated with beach slopes of 0.15, 0.12, 0.10, 0.08 and 0.05 are presented in Supplementary Figs. 6b, 7b and 8b.

Contributions of waves to water-level changes are sensitive to the beach slope parameter, but the overall results on the relative contribution of drivers of water-level changes are qualitatively robust in terms of spatial patterns and relative-contribution patterns. When the beach slope parameter decreases, the amplitude of water-level changes decreases due to the decrease in wave contributions to water-level changes (equations (1) and (2)). The opposite holds for an increase in the beach slope parameter. Wave set-up and swash remain dominant drivers of total water-level changes from extreme events to interannual-to-multidecadal changes and make substantial contributions to total water-level rise over large parts of the world's coasts regardless of the value used for the beach slope parameter.

Significance of the trends. The significance of the trend of each contributor, except tides (which are periodic), to total water-level changes at the coast relative to trends that could arise from natural climate interannual variability over the 23-year period is evaluated using a Monte Carlo method. We focus on trends induced by the two- to seven-year interannual variability, given the duration of our time series. It should, however, be noted that longer-term sea-level variations due to natural variability (such as the ENSO, PDO, Indian Ocean Dipole, North Atlantic Oscillation and other climate modes) could be substantial[62]. For each site and each contributor to total water-level changes at the coast, 10^4 random time series were generated with the same amplitude of interannual water-level changes as in our estimated contribution and using an autoregressive model of order 2 to model the autocorrelation in the two- to seven-year interannual variability[63]. For each site and each contributor, the distribution of the trends of the 10^4 time series was computed and the 0.95 percentile of the cumulative distribution was selected to provide the 95% confidence level for the significance of the trend (Supplementary Fig. 9a).

Trends of total water-level contributors (Fig. 4) are indistinguishable from trends induced by natural climate modes of variability at periods ranging from two to seven years if they are weaker (in absolute value) than the trends presented in Supplementary Fig. 9a. This analysis shows that in most places, excluding the northeastern Pacific coasts, the trend of the altimetry-derived sea level is significantly (at the 95% confidence level) different from trends arising solely from two- to seven-year natural climate variations (Supplementary Fig. 9b). Trends of other contributors are indistinguishable from trends induced by variability driven by natural climate modes, except for some wave components in the eastern tropical Pacific (Galápagos Islands and Tumaco) and at Honolulu and atmospheric surge at the Gothenburg tide gauge site in the Baltic (Supplementary Fig. 9b), although the last represents only a small contribution.

Data availability. The SSALTO/DUACS altimeter products were produced and distributed by the Copernicus Marine Environment Monitoring Service (http://marine.copernicus.eu/). Dynamical atmospheric corrections were produced by the *Collecte Localisation Satellites* Space Oceanography Division using the MOG2D model from *Laboratoire d'Etudes en Géophysique et Océanographie Spatiales* (LEGOS) and distributed by AVISO (Archiving, Validation and Interpretation of Satellite Oceanographic data), with support from *Centre National d'Etudes Spatiales* (CNES) (http://www.aviso.altimetry.fr/). FES2014 tidal data are produced by LEGOS. Tide gauge data were downloaded from the University of Hawaii Sea Level Center (https://uhslc.soest.hawaii.edu/data). ERA-Interim data were produced by the European Centre for Medium-Range Weather Forecasts (https://www.ecmwf.int/en/forecasts/datasets/reanalysis-datasets/era-interim).

References

51. Pujol, M. I. et al. DUACS DT2014: the new multi-mission altimeter data set reprocessed over 20 years. *Ocean Sci.* **12**, 1067–1090 (2016).
52. Merrifield, M. A., Becker, J. M., Ford, M. & Yao, Y. Observations and estimates of wave-driven water level extremes at the Marshall Islands. *Geophys. Res. Lett.* **41**, 7245–7253 (2014).
53. Ardhuin, F. & Roland, A. Coastal wave reflection, directional spread, and seismoacoustic noise sources. *J. Geophys. Res.* **117**, C00J20 (2012).
54. Idier, D., Paris, F., Le Cozannet, G., Boulahya, F. & Dumas, F. Sea-level rise impacts on the tides of the European Shelf. *Cont. Shelf Res.* **137**, 56–71 (2017).
55. Stopa, J. E. & Cheung, K. F. Intercomparison of wind and wave data from the ECMWF Reanalysis Interim and the NCEP Climate Forecast System Reanalysis. *Ocean Model.* **75**, 65–83 (2014).
56. Wang, X. L. & Swail, V. R. Climate change signal and uncertainty in projections of ocean wave heights. *Clim. Dyn.* **26**, 109–126 (2006).
57. Hemer, M. A. Historical trends in Southern Ocean storminess: long-term variability of extreme wave heights at Cape Sorell, Tasmania. *Geophys. Res. Lett.* **37**, L18601 (2010).
58. Komar, P. *Beach Processes and Sedimentation*. 2nd ed. (Prentice Hall, Upper Saddle River, 1998).
59. Holman, R. & Sallenger, A. Setup and swash on a natural beach. *J. Geophys. Res.* **90**, 945–953 (1985).
60. Stockdon, H. F. & Holman, R. A. Estimation of wave phase speed and nearshore bathymetry from video imagery. *J. Geophys. Res.* **105**, 22015–22033 (2000).
61. Di Leonardo, S. & Ruggiero, P. Regional scale sandbar variability: observations from the US Pacific Northwest. *Cont. Shelf Res.* **95**, 74–88 (2015).
62. Dangendorf, S. et al. Evidence for long-term memory in sea level. *Geophys. Res. Lett.* **41**, 5530–5537 (2014).
63. Von Storch, H. & Zwiers, F. *Statistical Analysis in Climate Research* (Cambridge Univ. Press, Cambridge, 1999).

SUPPLEMENTARY INFORMATION
https://doi.org/10.1038/s41558-018-0088-y

nature climate change

In the format provided by the authors and unedited.

Under-estimated wave contribution to coastal sea-level rise

Angélique Melet[1*], Benoit Meyssignac[2], Rafael Almar[2] and Gonéri Le Cozannet[3]

[1]Mercator Ocean, Ramonville Saint Agne, France. [2]LEGOS, Université de Toulouse, CNES, CNRS, IRD, UPS, Toulouse, France. [3]BRGM / French Geological Survey, Orléans, France. *e-mail: amelet@mercator-ocean.fr

SUPPLEMENTARY INFORMATION

Underestimated wave contribution to coastal sea level rise

Angélique Melet[1,*], Benoit Meyssignac[2], Rafael Almar[2], Gonéri LeCozannet[3]

1. Mercator Ocean, Ramonville St Agne, France

2. LEGOS, Université de Toulouse, CNES, CNRS, IRD, UPS, Toulouse, France

3. BRGM/French Geological Survey, Orléans, France

Contact information:

Dr. Angélique Melet

8-10 rue Hermès

31520 Ramonville Saint-Agne

France

amelet@mercator-ocean.fr

Supplementary Information

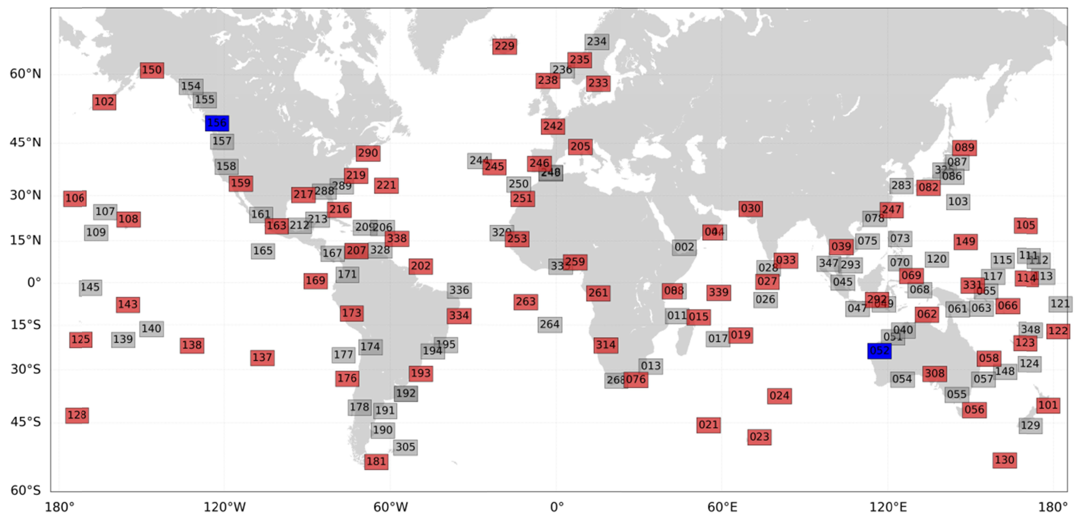

Supplementary Figure 1 | Location of the coastal sites. Coastal sites for which results are shown in the main text (Figures 2, 3, 4) are in red. Coastal sites for which time-series of the contributors to total water-level changes at the coast are provided in Supplementary Figures 2 and 3 are in blue (Carnarvon, Australia: index 052; Tofino, Canada: index 156).

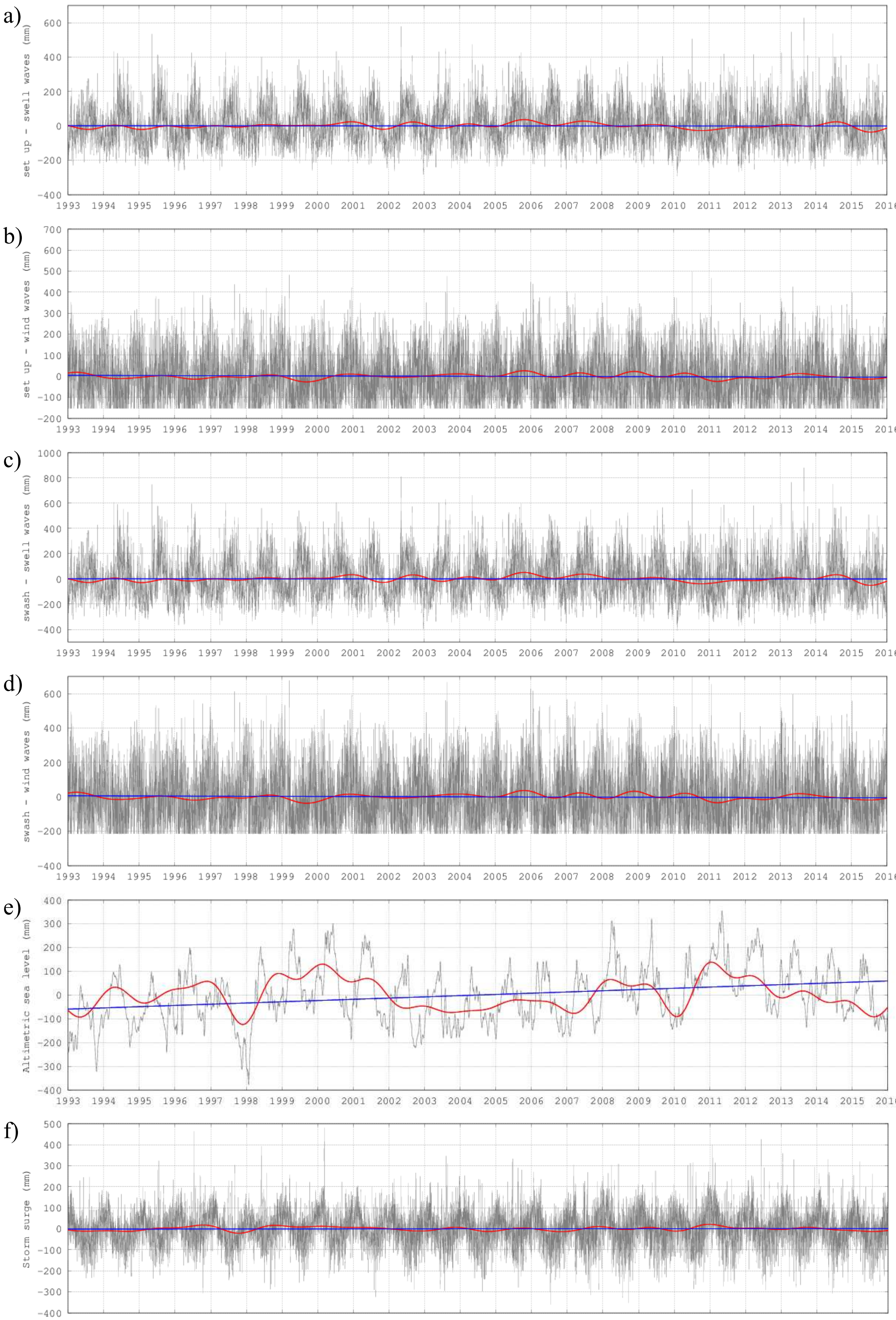
a)
set up - swell waves (mm)
b)
set up - wind waves (mm)
c)
swash - swell waves (mm)
d)
swash - wind waves (mm)
e)
Altimetric sea level (mm)
f)
Storm surge (mm)
1993 1994 1995 1996 1997 1998 1999 2000 2001 2002 2003 2004 2005 2006 2007 2008 2009 2010 2011 2012 2013 2014 2015 2016

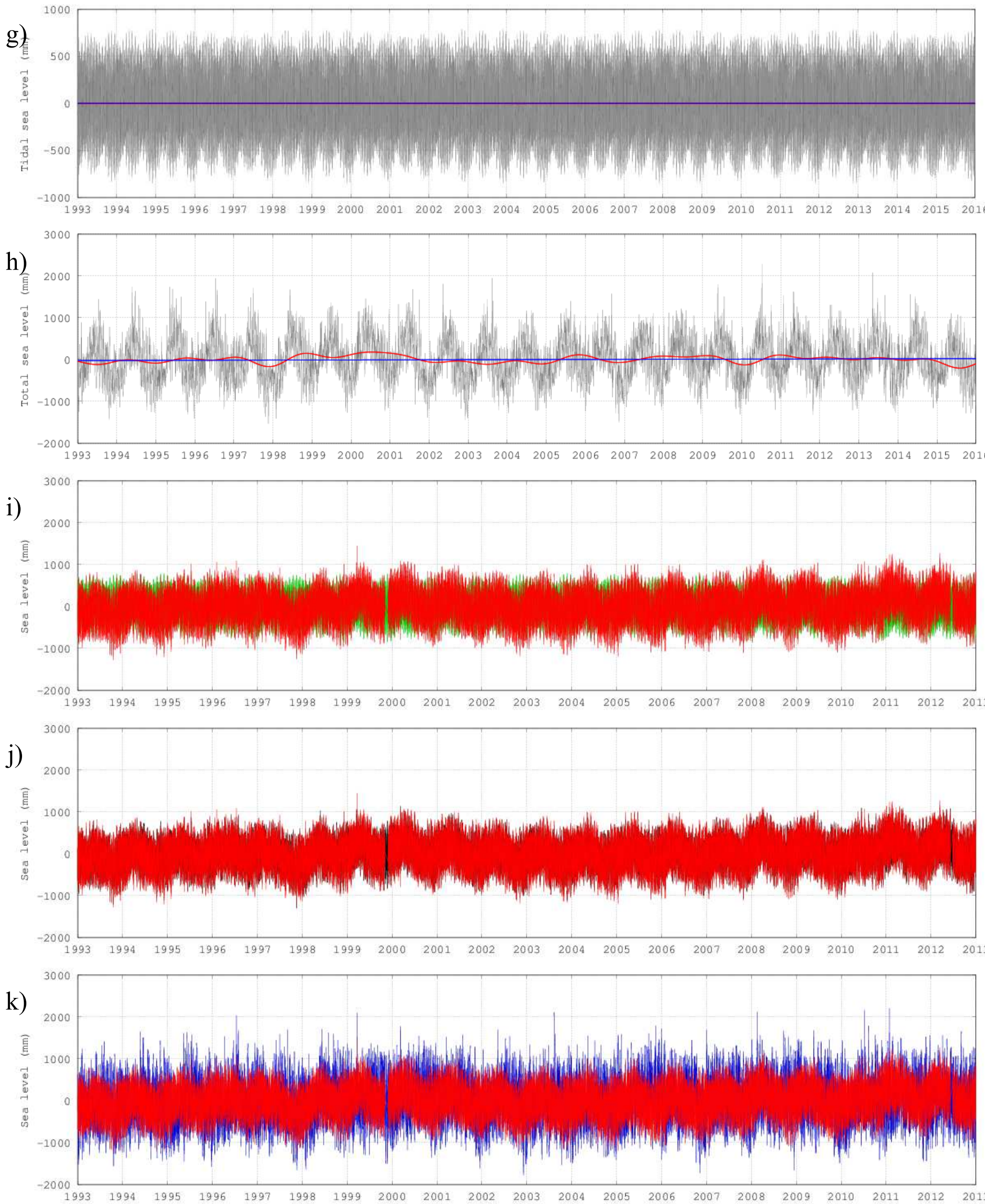

Supplementary Figure 2 | Time-series of the contributors to total water-level changes at the coast at Carnarvon (Australia, 24.90°S, 113.65°E, index 052 in Supplementary Figure 1) and comparison of water-level to the tide gauge record. Time-series of the different contributors to total water-level changes (anomalies relative to the 1993–2015 mean, in mm): (a) swell-waves set-up, (b) wind-waves set-up, (c) swell-waves swash, (d) wind-waves swash, (e) altimetric sea level, (f) atmospheric surge, (g) tides, (h) sum of all contributors (a to g) at a daily resolution. In panels (a) to (h), the time-series is shown in grey, the linear regression (trend) in blue and the interannual variability of the detrended time-series in red. (i) to (k) Comparison to tide gauge data. The tide gauge data is shown in red. Time-series of (i) tides (in green), (j) the sum of contributors to water-level changes but excluding wave contributions (in black), (k) the sum of all contributors to water-level changes, including wave contributions (i.e. total water-level, in blue). Note the different scales for each panel.

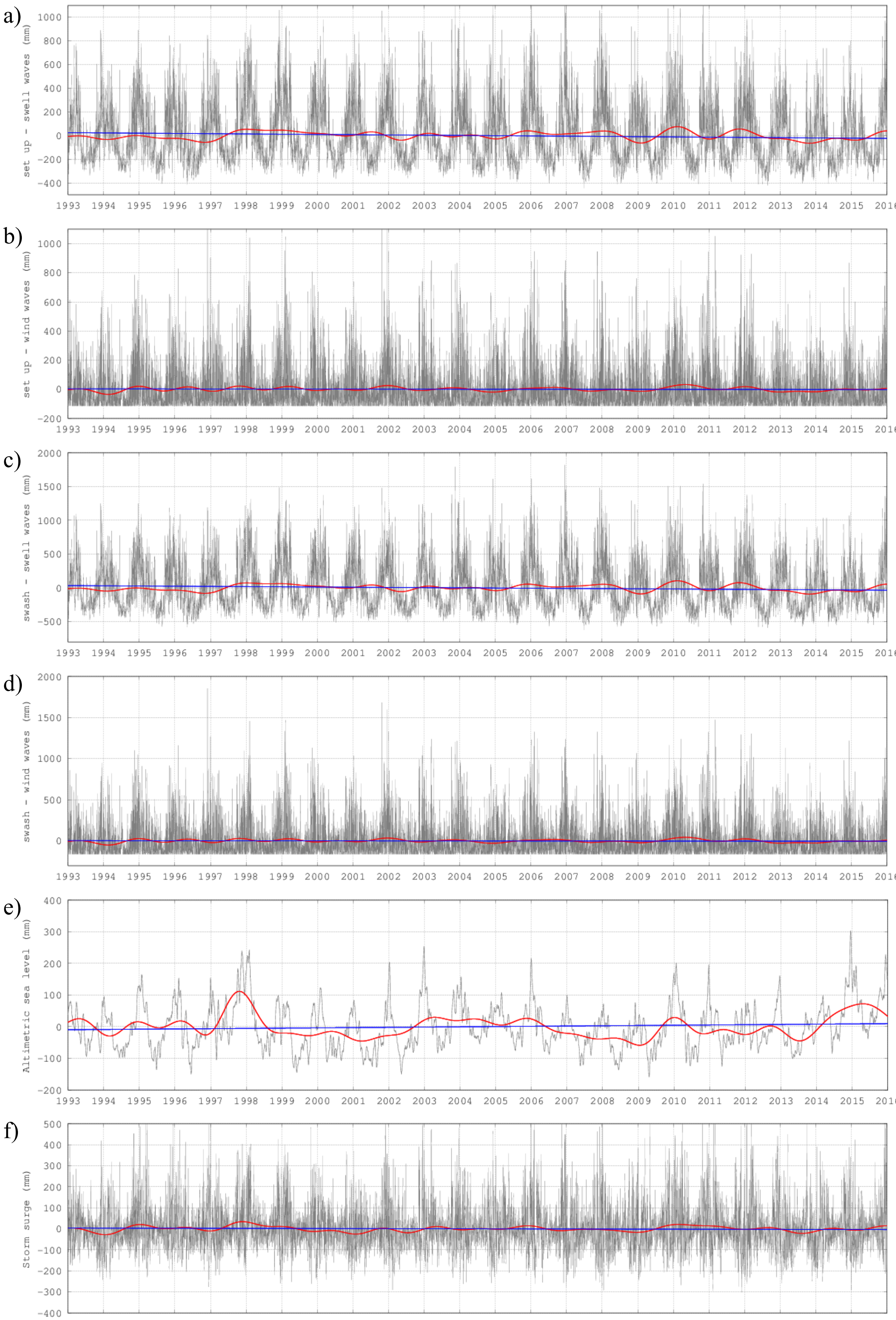
a)
set up - swell waves (mm)
b)
set up - wind waves (mm)
c)
swash - swell waves (mm)
d)
swash - wind waves (mm)
e)
Altimetric sea level (mm)
f)
Storm surge (mm)
1993 1994 1995 1996 1997 1998 1999 2000 2001 2002 2003 2004 2005 2006 2007 2008 2009 2010 2011 2012 2013 2014 2015 2016

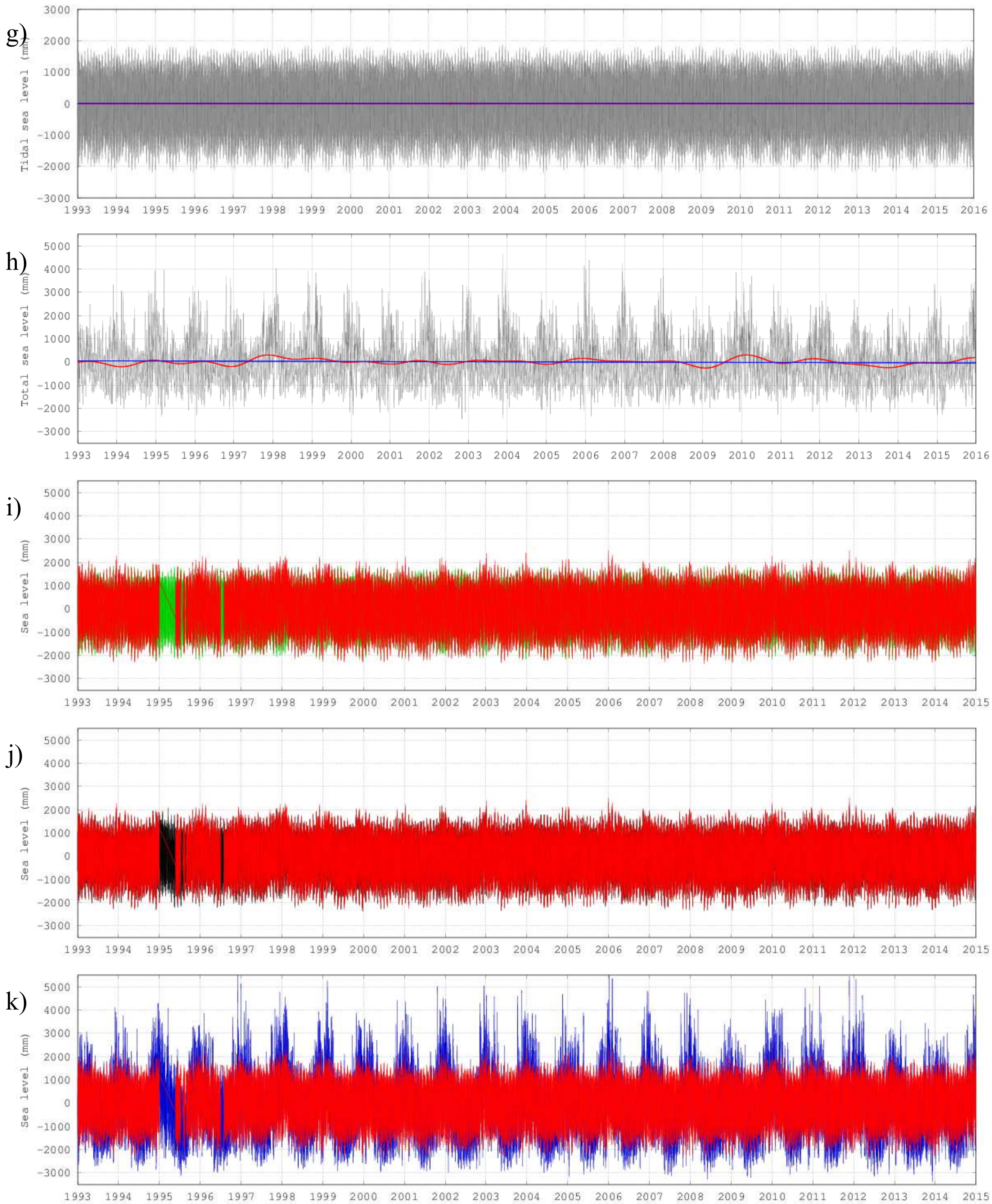

Supplementary Figure 3 | Time-series of the contributors to sea level changes at the coast at Tofino (Canada, 49.19°N 125.92°W, index 156 in Supplementary Figure 1) and comparison of sea level to the tide gauge record. (a) Time-series of the different contributors to sea level changes (anomalies relative to the 1993–2015 mean, in mm): (a) swell-waves set-up, (b) wind-waves set-up, (c) swell-waves swash, (d) wind-waves swash, (e) altimetric sea level, (f) atmospheric surge, (g) tides, (h) sum of all contributors (a to g) at a daily resolution. In panels (a) to (h), the time-series is shown in grey, the linear regression (trend) in blue and the interannual variability of the detrended time-series in red. (i) to (k) Comparison to tide gauge data. The tide gauge data is shown in red. Time-series of (i) tides (in green), (j) the sum of contributors to sea level changes but excluding wave contributions (in black), (k) the sum of all contributors to sea level changes, including wave contributions (in blue). Note the different scales for each panel.

a)

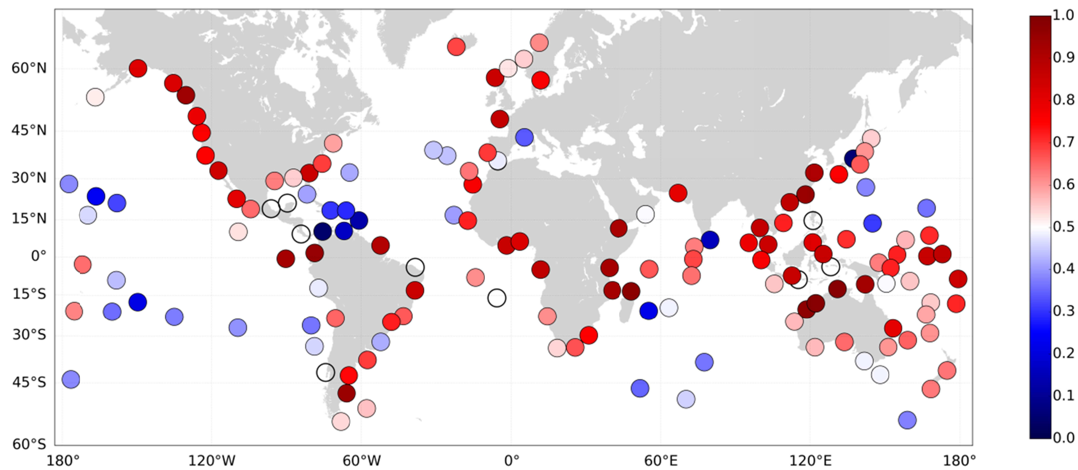

60°N
45°N
30°N
15°N
0°
15°S
30°S
45°S
60°S
180°
120°W
60°W
0°
60°E
120°E
180°
1.0
0.9
0.8
0.7
0.6
0.5
0.4
0.3
0.2
0.1
0.0

b)

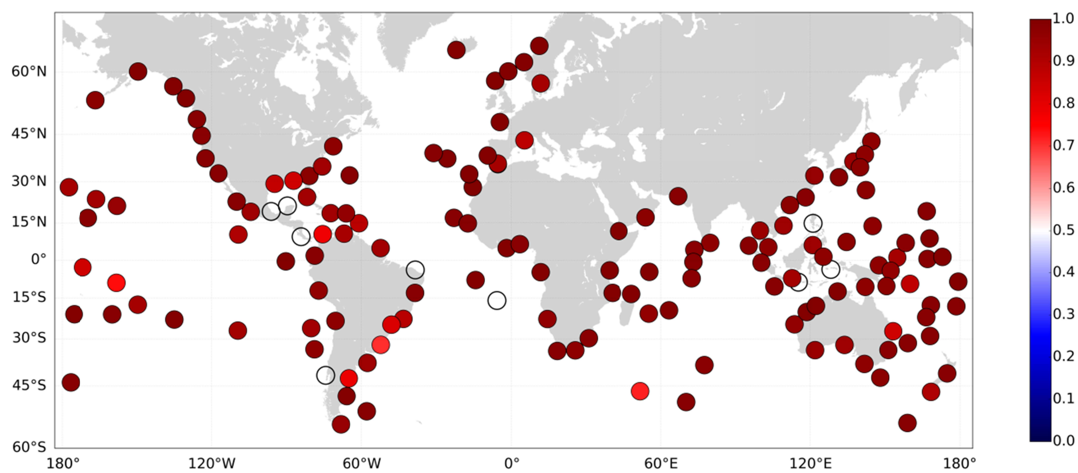

60°N
45°N
30°N
15°N
0°
15°S
30°S
45°S
60°S
180°
120°W
60°W
0°
60°E
120°E
180°
1.0
0.9
0.8
0.7
0.6
0.5
0.4
0.3
0.2
0.1
0.0

c)

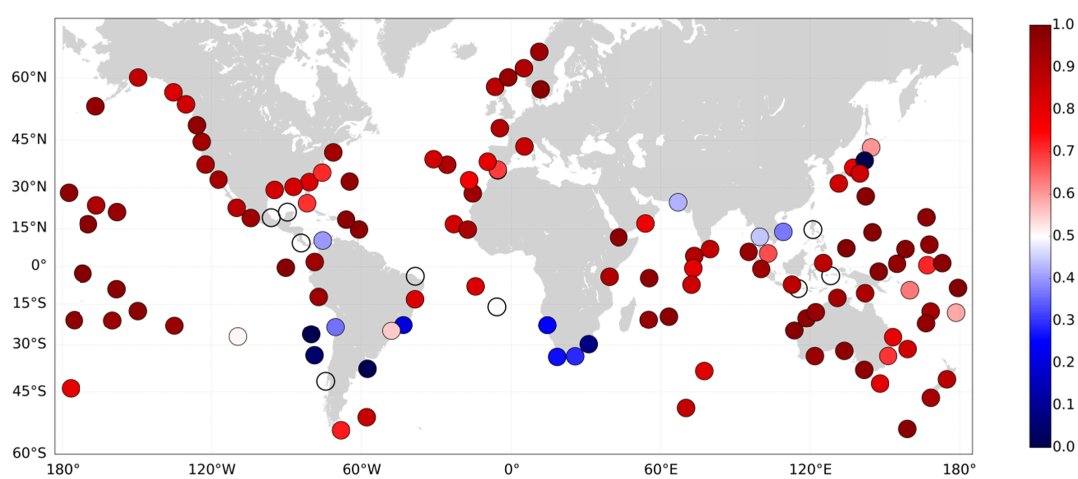

60°N
45°N
30°N
15°N
0°
15°S
30°S
45°S
60°S
180°
120°W
60°W
0°
60°E
120°E
180°
1.0
0.9
0.8
0.7
0.6
0.5
0.4
0.3
0.2
0.1
0.0

Supplementary Figure 4 | Correlation of tide gauge records with the sum of water-level contributions at the coast. (a) Estimates of water-level at the coast, including the contributions from waves (wind-wave and swell) set-up and swash (i.e. total water-level) and considering all time scales. (b) Estimates of water-level at the coast, excluding the contributions from wave set-up and swash and considering all time scales. (c) Estimates of water-level at the coast, excluding the contributions from wave set-up and swash and considering interannual-to-multidecadal time scales only.

In each panel, empty circles correspond to tide gauge records with leveling issues, so that no correlation is provided. Durations of the tide gauge records are site dependent.

a)

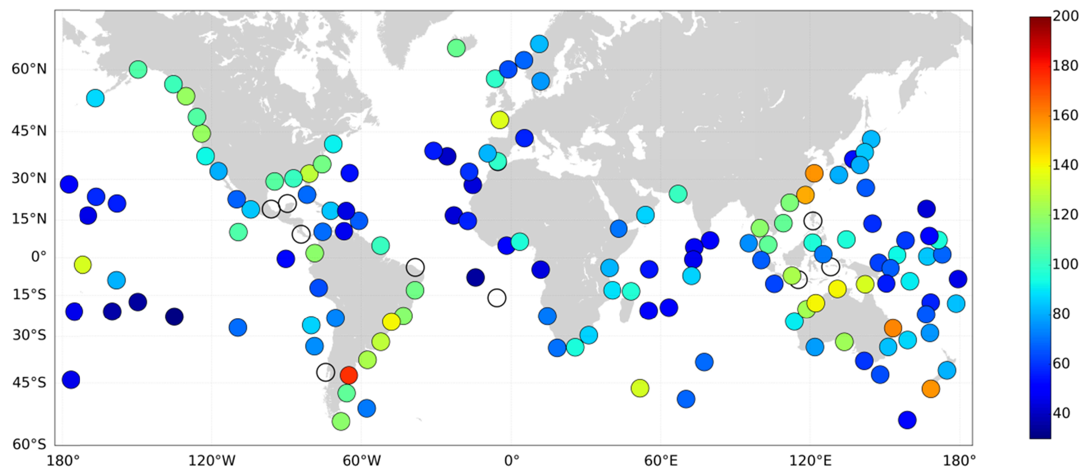

b)

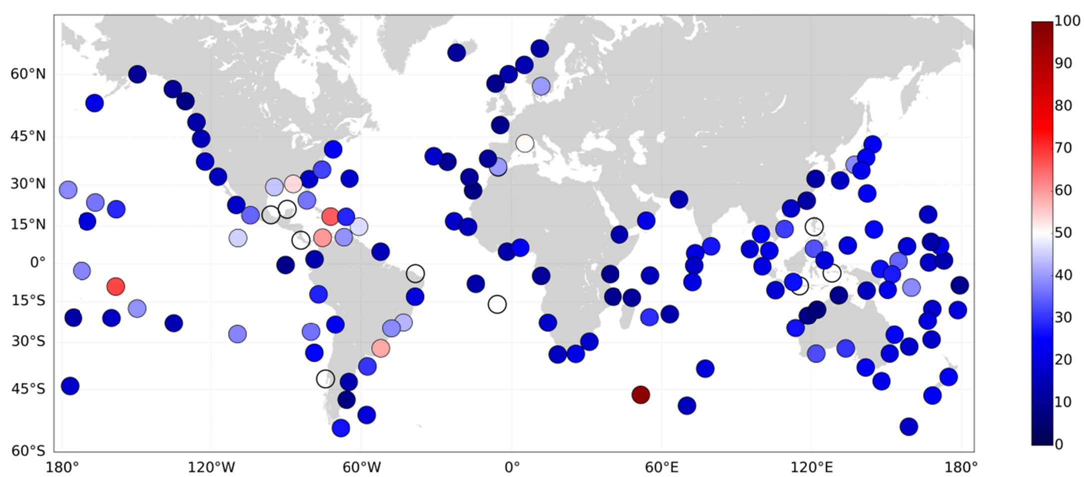

Supplementary Figure 5 | Comparison to tide gauges. (a) Root mean square of the differences between the sum of water-level contributions at the coast and tide-gauge records considering all time scales (in mm). (b) Percentage of the root mean square of the water-level estimates over the tide gauge record periods represented by the root mean square differences between the water-level estimates and the tide gauge records (shown in (a)). Estimates of water-level at the coast exclude the contributions from waves. Empty circles correspond to tide gauge records with leveling issues, so that no value is provided. Durations of the tide gauge records are site dependent.

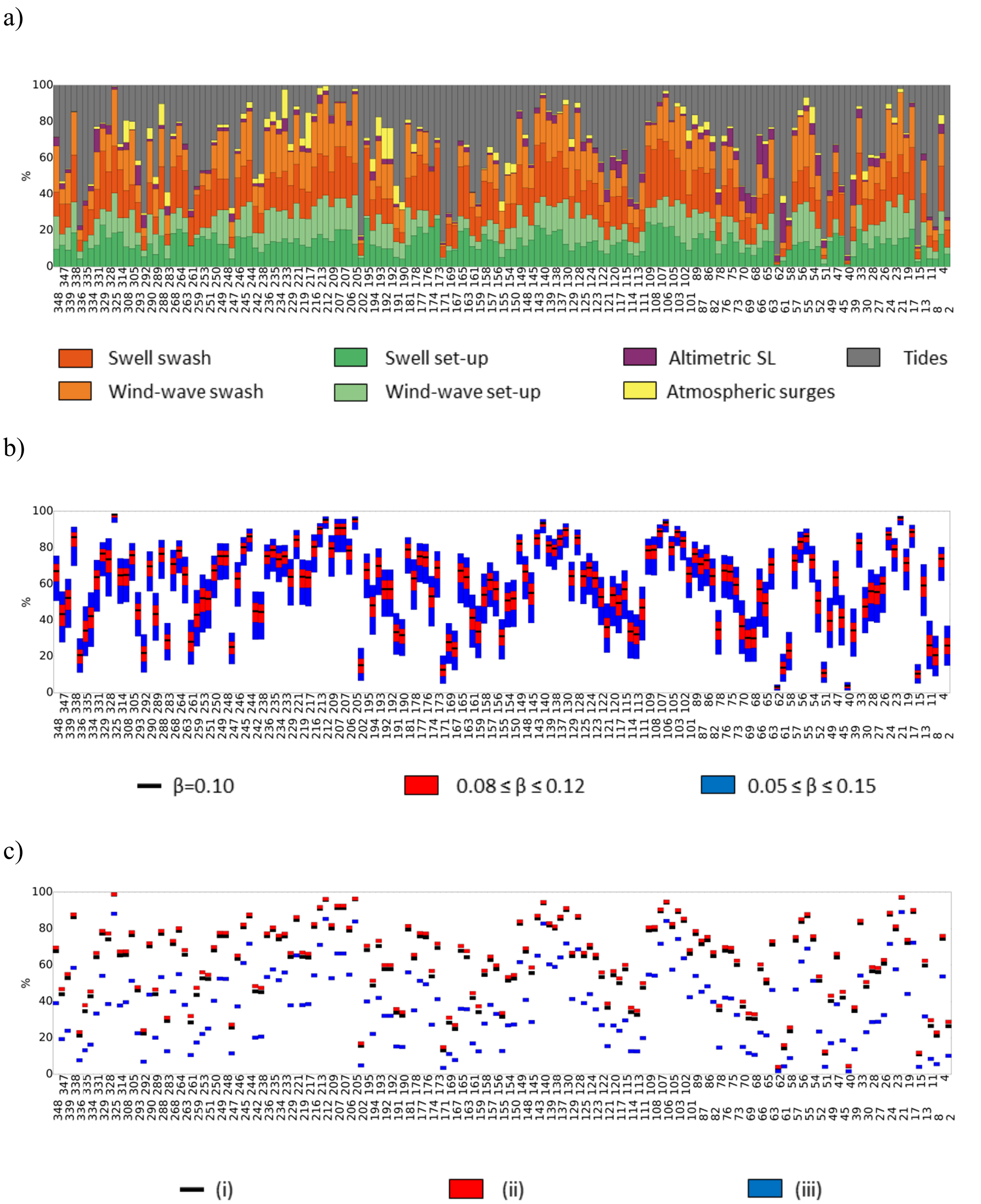

Supplementary Figure 6 | Contributions to extreme total-water levels. (a) Percentage of extreme total water-levels variance represented by each contributor at each of the 153 coastal sites (swell swash in dark orange, wind-wave swash in light orange, swell set-up in dark green, wind-wave set-up in light green, altimetry-derived sea level in violet, atmospheric surges in yellow, tides in grey). The beach slope is set to 0.1 and wave set-up and swash are estimated with formulation (i) as in the main text. (b) Sensitivity of the percentage of extreme total water-levels variance represented by the sum of wave contributions (sum of swell and wind-wave set-up and swash) to the beach slope parameter. The relative contribution of waves using a beach slope of 0.10 is shown in black, relative contributions of waves using beach slopes of 0.12 and 0.08 are delineated in red, relative contributions of waves using beach slopes of 0.15 and 0.05 are delineated in blue. (c) Sensitivity of the percentage of extreme total water-levels variance represented by the sum of wave contributions (sum of swell and wind-wave set-up and swash) to the formulation used to estimate wave set-up and swash. Results for formulation (i) are shown in black, results for formulation (ii) are shown in red and results for formulation (iii) are shown in blue.

Indices on the bottom of each panel are the indices of the tide gauge records as shown in Supplementary Figure 1.

a)

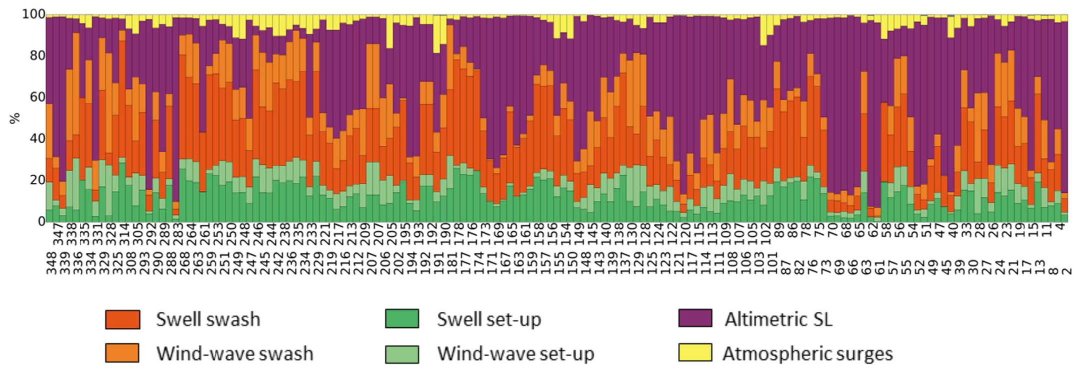

b)

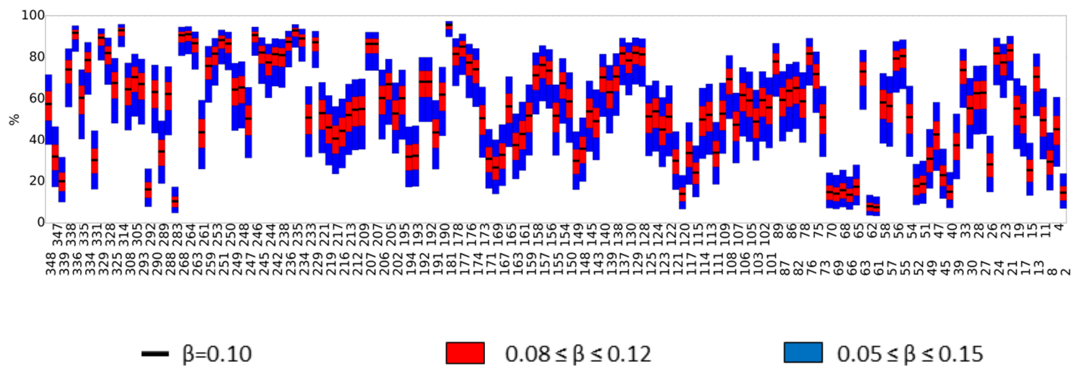

c)

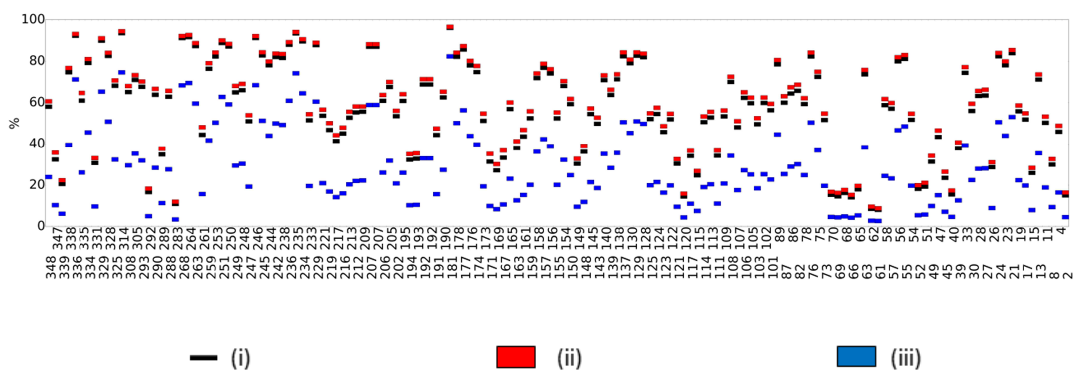

Supplementary Figure 7 | Contributions to detrended interannual-to-multidecadal total-water levels. (a) Percentage of interannual-to-multidecadal total water-level variance represented by each contributor at each of the 153 coastal sites (swell swash in dark orange, wind-wave swash in light orange, swell set-up in dark green, wind-wave set-up in light green, altimetry-derived sea level in violet, atmospheric surges in yellow). The beach slope is set to

0.1 and wave set-up and swash are estimated with formulation (i) as in the main text. (b) Sensitivity of the percentage of interannual-to-multidecadal total water-level variance represented by the sum of wave contributions (sum of swell and wind-wave set-up and swash) to the beach slope parameter. The relative contribution of waves using a beach slope of 0.10 is shown in black, relative contributions of waves using beach slopes of 0.12 and 0.08 are delineated in red, relative contributions of waves using beach slopes of 0.15 and 0.05 are delineated in blue. (c) Sensitivity of the percentage of interannual-to-multidecadal total water-level variance represented by the sum of wave contributions (sum of swell and wind-wave set-up and swash) to the formulation used to estimate wave set-up and swash. Results for formulation (i) are shown in black, results for formulation (ii) are shown in red and results for formulation (iii) are shown in blue.

Indices on the bottom of each panel are the indices of the tide gauge records as shown in Supplementary Figure 1.

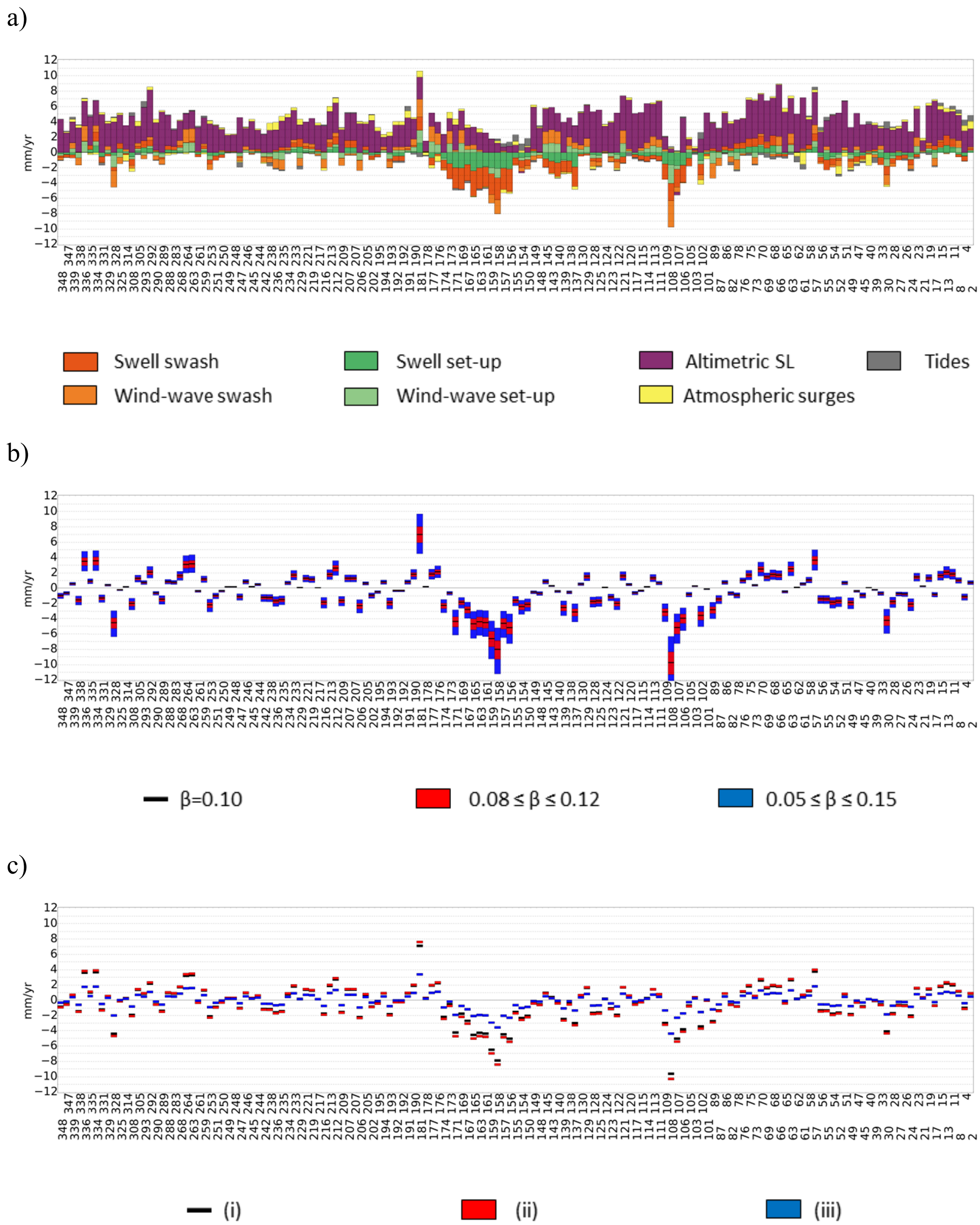

Supplementary Figure 8 | Contributions to total-water level trends. (a) Trends of each contributor to total water-levels at each of the 153 coastal sites (swell swash in dark orange, wind-wave swash in light orange, swell set-up in dark green, wind-wave set-up in light green, altimetry-derived sea level in violet, atmospheric surges in yellow, tides in grey). The beach slope is set to 0.1 and wave set-up and swash are estimated with formulation (i) as in the main text. (b) Sensitivity of trends of the sum of wave contributions (sum of swell and wind-wave set-up and swash) to the beach slope parameter. Trends of the wave contribution using a beach slope of 0.10 is shown in black, trends of the wave contribution using beach slopes of 0.12 and 0.08 are delineated in red, trends of the wave contribution using beach slopes of 0.15 and 0.05 are delineated in blue. (c) Sensitivity of trends of the sum of wave contributions (sum of swell and wind-wave set-up and swash) to the formulation used to estimate wave set-up and swash. Results for formulation (i) are shown in black, results for formulation (ii) are shown in red and results for formulation (iii) are shown in blue.

Indices on the bottom of each panel are the indices of the tide gauge records as shown in Supplementary Figure 1.

a)

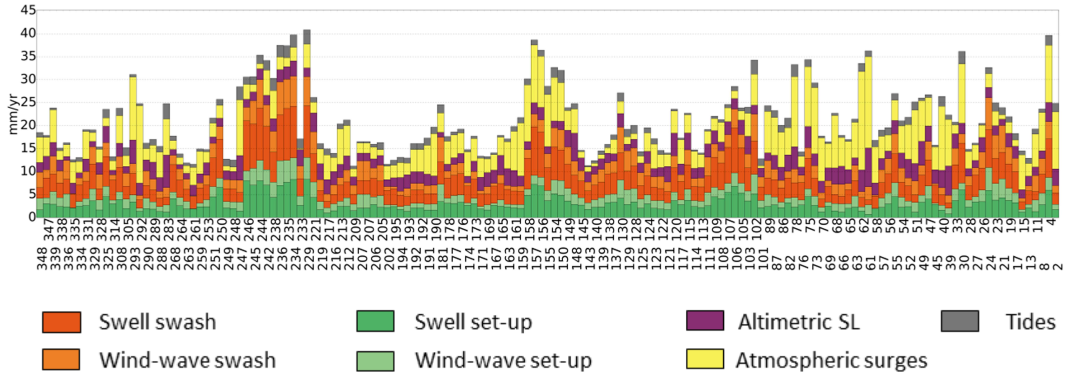

b)

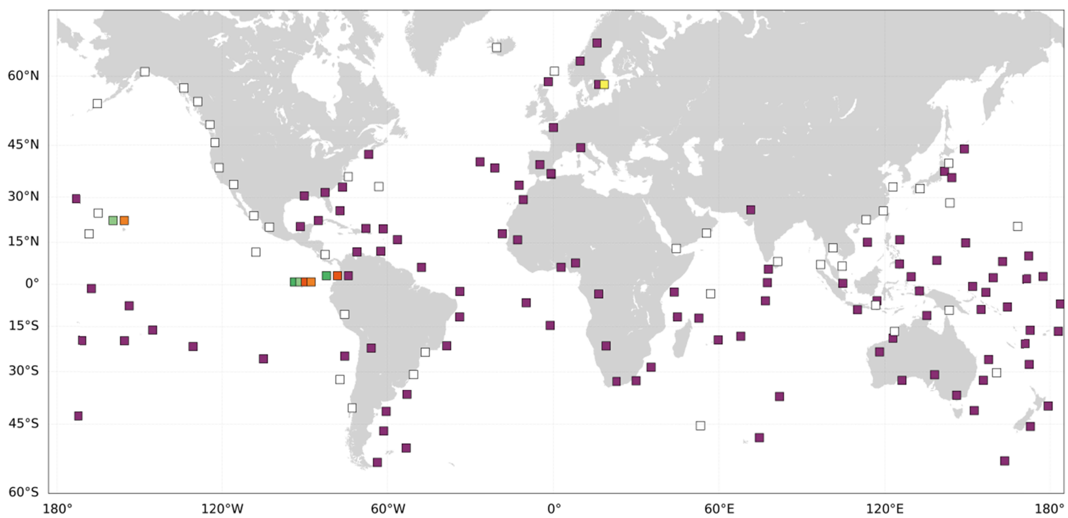

Supplementary Figure 9 | Significance of the trends relative to trends that could arise from natural climate interannual variability only. (a) 95% confidence level of trends induced by natural variability (random fluctuations with red noise modelled with an order 2 auto-regressive process to take into account the autocorrelation in time series) at interannual time-scales for each contributor to total water-level trends at the coast (swell swash in dark orange, wind-wave swash in light orange, swell set-up in dark green, wind-wave set-up in light green, altimetry-derived sea level in violet, atmospheric surges in yellow, tides in grey). (b) Contributors for which the trend (shown in Figure 4) is larger (in absolute value) than the 95% confidence level trend induced by natural interannual variability (panel a) are shown in color for each site: swell swash in dark orange, wind-wave swash in light orange, swell set-up in dark green, wind-wave set-up in light green, altimetry-derived sea level in violet, atmospheric surges in yellow. Sites with a white box are sites for which none of the contributors to total water-level trend at the coast has a significant trend at the 95% confidence level.

Supplementary Note | Contributions to extreme events.

Our estimated contributions to extreme events are overall dominated by waves and tides (Figure 2, Supplementary Figure 6), which is consistent with previous studies. Although not accounted for in most global studies focused on extreme events, swash is the dominant contributor to total water-level extreme along open coasts located close to our network of tide gauges. Wave set-up also shows a large contribution. Regional patterns arise regarding the relative importance of the different contributions: extreme events are of highest amplitude and mostly due to both wind-waves and swells at mid-to-high latitudes (Europe, Northern America, Japan, Southern Ocean, and southern South America) (Figure 2). These regions correspond to coasts exposed to storms, high local winds and wave heights. In the tropics, extreme events have lower amplitudes, but are still a threat for the coastal population as the relative departure during extremes from usual conditions (e.g. variations below the 98% percentile) is of similar amplitude in the tropics and at higher latitudes (not shown). Wave contributions to extreme events in the tropics tend to be smaller than at mid-to-high latitudes and tides have a more dominant role, meaning that extreme levels primarily occur during spring tides. Components measured by satellite altimetry (Figure 1) have a non-negligible contribution to extreme events in the western tropical Pacific, while the contribution from atmospheric surges is significant at coastal locations facing large continental shelves (e.g. Baltic and North Seas, Argentina's coast, Figure 2).